NANO LETTERS

Letter

pubs.acs.org/NanoLett

Strings-to-Rings Transition and Antiparallel Dipole Alignment in Two-Dimensional Methanols

Ronen Zangi*[,†,‡] and Danilo Roccatano[§,∥]

[†]Polymat & Department of Organic Chemistry I, University of the Basque Country UPV/EHU, Avenida de Tolosa 72, 20018 San Sebastian, Spain

[‡]IKERBASQUE, Basque Foundation for Science, Maria Diaz de Haro 3, 48013 Bilbao, Spain

[§]School of Mathematics and Physics, University of Lincoln, Brayford Pool, Lincoln LN6 7TS, U.K.

[∥]School of Engineering and Science, Jacobs University Bremen, Campus Ring 1, 28759 Bremen, Germany

Supporting Information

ABSTRACT: Structural order emerging in the liquid state necessitates a critical degree of anisotropy of the molecules. For example, liquid crystals and Langmuir monolayers require rod- or disc-shaped and long-chain amphiphilic molecules, respectively, to break the isotropic symmetry of liquids. In this Letter we present results from molecular dynamics simulations demonstrating that in two-dimensional liquids, a significantly smaller degree of anisotropy is sufficient to allow structural organization. In fact, the condensed phase of the smallest amphiphilic molecule, methanol, confined between two, or adsorbed on, graphene sheets forms a monolayer characterized by long chains of molecules. Intrachain interactions are dominated by hydrogen bonds, whereas interchain interactions are dispersive. Upon a decrease in density toward a gaslike state, these strings are transformed into rings. The two-dimensional liquid phase of methanol undergoes another transition upon cooling; in this case, the order−disorder transition is characterized by a low-temperature phase in which the hydrogen bond dipoles of neighboring strings adopt an antiparallel orientation.

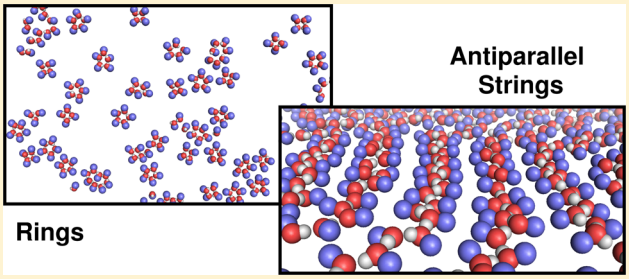

KEYWORDS: *Two-dimensional system, fluids under confinement, order−disorder transition, self-organization, amphiphilic molecules*

It is well-known that in two-dimensional (2D) systems thermal fluctuations can completely suppress long-range translational order.[1,2] Furthermore, the balance between the changes in entropy and enthalpy across the transition from the isotropic liquid to the ordered crystalline state is not equal to its three-dimensional (3D) counterpart, impeding or promoting the freezing transition. The behavior in reduced dimensionality can be also coupled to the chemical or shape anisotropy of the molecules. Water under different confinements has been subject to many investigations;[3−8] however, it is lacking any significant degree of anisotropy. One of the simplest anisotropic molecules is methanol. As of yet, its liquid state in confined geometries has been studied only inside cylindrical nanotubes.[9−17]

In this work we investigated monolayers of methanols that are either confined between two graphenes or freely adsorbed on a single graphene sheet. Figure 1 displays the fraction of methanol molecules participating in strings (chains) and rings structural elements. In the condensed phase at high densities, the methanols are organized predominantly in chains of molecules in which each methanol inside the chain accepts one hydrogen bond and donates another. As the density is decreased toward the gas phase, these strings are transformed into rings. Figure 2 exhibits three instantaneous configurations of the simulation box along this transition. The "backbone" of these strings and rings is a sequence of hydrogen bonds between the hydroxyl groups. There are also, albeit weaker, dispersion interactions between adjacent methyl groups. The latter, nonetheless, are responsible for the interactions between the structural elements. At intermediate densities (e.g., ρ_{2D} = 2.88 nm^{-2}), strings coexist alongside rings; however, no phase separation was observed in any of the systems studied. Figures S1 and S2a in the Supporting Information indicate that the average length of the strings rises linearly as the 2D density increases, with values in the range of 4−13 molecules long, and exhibits a maximum around ρ_{2D} = 5.76 and 4.80 nm^{-2} for the confined and adsorbed systems, respectively. In comparison, the average chain length of bulk methanol was found to be 2.7 molecules.[18] In contrast to the behavior of strings, four- and five-member rings are by far the most abundant ring sizes and are barely affected by the 2D density (Figure S2b and Table S1).

Apart from the difference in the shape and size of the two motifs, strings and rings differ also in the way the methanol

Received: February 2, 2016
Revised: March 30, 2016
Published: March 30, 2016

DOI: 10.1021/acs.nanolett.6b00460
Nano Lett. 2016, 16, 3142−3147

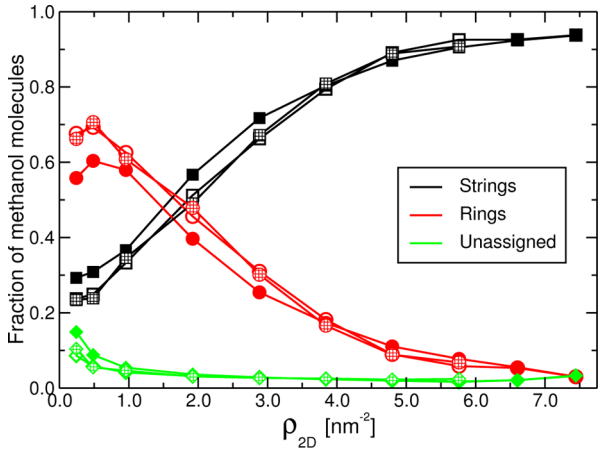

Figure 1. Density-induced strings-to-rings transition. The fractions of methanols participating in strings (black squares) or rings (red circles) structural elements as a function of their 2D-density (see Experimental Section for details) are shown. The fraction of particles that do not fit to either of these definitions is also displayed (green diamonds). In these simulations, the temperature, T = 300 K, and the area of a graphene sheet, A = 148.4 nm^2, are held constant. Filled and empty symbols are results from methanols confined between two graphene sheets 0.83 nm apart in which the electrostatic interactions were calculated by the PME and cutoff methods, respectively. Symbols filled with square pattern are results from cutoff simulations of methanols adsorbed onto a single graphene.

molecules are arranged with respect to one another along the structural motif. In general, strings are composed of chains of methanols in which the methyl groups of neighboring molecules point in opposite directions, forming a zigzag pattern. Obviously, at finite temperature this pattern is subject to defects as shown in a snapshot in Figure S3a taken from a simulation at T = 300 K. With a decrease in temperature, there is a reduction of these defects as demonstrated in Figure S3b. In this case, the only defect from a perfect zigzag arrangement permits the chain to adopt a kink. In fact, infinitely long zigzag chains of molecules have been reported to occur in the crystal structure of methanol in three dimensions,[19−22] as well as in a monolayer film adsorbed on graphite.[23] In contrast to strings, rings are arranged by methanols pointing their methyl groups only outward (Figure S3c,d). As is the case for the defect mentioned above, when the methyl groups reside on the same side, their excluded volumes force a bend in the linear chain and consequently induce formation of a circular shape.

Why do strings appear at high densities and rings at low densities? The packing efficiency of strings is higher than that of rings; therefore, they are found at higher 2D densities. At lower densities approaching the gas phase, the entropy of the particles is a dominant factor dictating its phase state. Thus, the methanol molecules will tend to maximize the number of independent structural elements. Short strings with only one hydrogen bond at the edges pose a large enthalpic penalty relative to their size. A way to circumvent that is to form rings. The most probable sizes observed of four- and five-member rings are likely to be a consequence of the balance between the strain of the ring and the tendency to maximize their number.

In a series of simulations in which we varied the temperature at a fixed 2D density in the condensed phase (ρ_{2D} = 5.76 nm^{-2}), our algorithm for the calculations of structural elements found that at lower temperatures the fraction of rings increases on the expense of strings. However, visual inspections of these rings identified them as actually large strings in which both ends are connected (see Figure S3e). We arrived to this conclusion because the methanols in these "rings" are arranged in a zigzag structure and their packing efficiency is large, properties characterizing strings. Even in the absence of a quantified descriptor, it is clear that at lower temperatures the lengths of the strings increases. However, a more interesting observation is that upon lowering the temperature another transition is found.

In forming a chain of hydrogen bonds, the dipole moments of the −OH covalent bonds, or alternatively the dipole moments of the hydrogen bonds themselves, are all aligned in the same direction. Neighboring chains can then adopt any orientation with respect to this chain. This is indeed the case at high temperature. However, at low temperatures we find a phase characterized by chains oriented antiparallel to their nearest neighbor chains.

To quantify this order−disorder transition we defined an order parameter, Φ, that measures the angle between the −OH covalent bonds of neighboring methanols that belong to different chains. A random distribution of the hydroxyl dipoles corresponds to Φ = 0, whereas, perfect parallel and antiparallel organizations correspond to Φ = +1 and Φ = −1, respectively. The value of Φ as a function of temperature is shown in Figure 3. At high temperatures, the magnitude of Φ is small; however, Φ is always on the negative side. This suggests a nearly complete absence of correlations between the orientations of −OH dipoles of different chains. With a decrease in temperature, there is a clear transition toward a state characterized by a large negative value of Φ, pointing to the antiparallel alignments of the −OH covalent bonds of neighboring chains. Figure 3 also indicates an almost complete lack of order in bulk methanol at all temperatures.

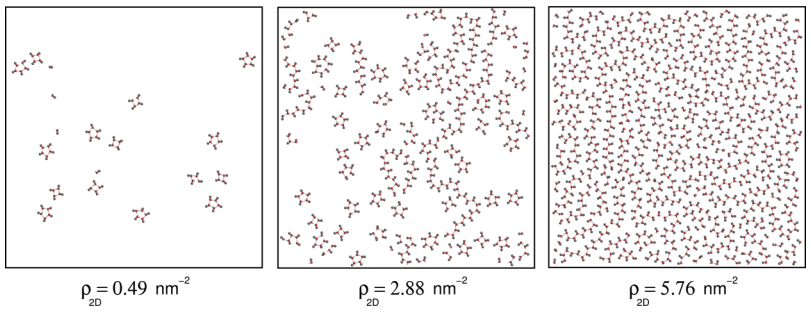

Figure 2. Snapshots from the confined simulations analyzed in Figure 1 at three different 2D densities (nm^{-2}) spanning the strings-to-rings transition. The methyl groups, oxygens, and hydrogens are depicted in gray, red, and white, respectively. The confining graphene sheets are not shown for clarity.

DOI: 10.1021/acs.nanolett.6b00460
Nano Lett. 2016, 16, 3142−3147

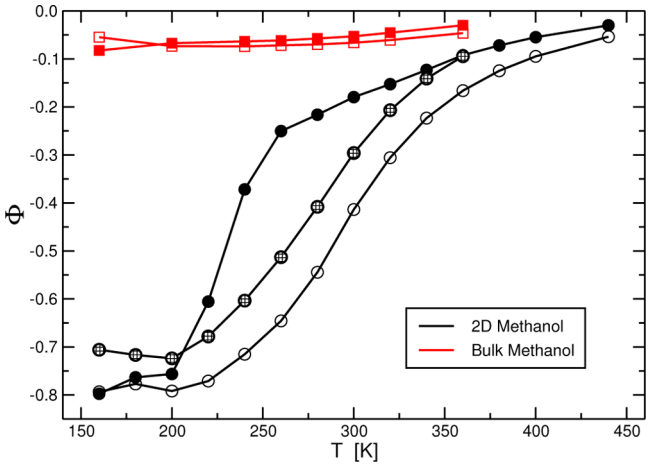

Figure 3. Temperature-induced antiparallel alignment of strings. The order parameter, Φ, measuring the antiparallel orientation of the −OH covalent bonds of non-hydrogen-bonded nearest neighbor methanols, is shown as a function of temperature. The three types of 2D methanol systems (three types of black circles) are the same as those described in Figure 1 for ρ_{2D} = 5.76 nm^{-2}. Values obtained for bulk methanol (red squares) are shown for comparison (where filled and empty symbols have the same meanings as in the 2D systems). Φ is defined by $\Phi = \left\langle \frac{1}{N} \sum_{i=1}^{N} \cos \theta_i \right\rangle$ where the sum is performed over all N methanol molecules and the angle brackets denote ensemble average. θ_i is the angle between the −OH covalent bonds of particle i and its non-hydrogen-bonded nearest neighbor. The latter is identified by the shortest distance between the methyl groups excluding the first three hydrogen-bonded neighbors toward each direction of the chain.

The antiparallel alignment of the hydrogen bond direction of neighboring chains is shown in a close-up snapshot in the top panel of Figure 4. In the lower panel, snapshots at three different temperatures along the transition are shown. Here the dipole moments of the methanol molecules are colored according to their orientations. The driving force for this ordering is the gain in energy from dipole−dipole interactions. We analyzed in Figure S4a the energy between the methanol molecules as a function of temperature. The shape of the curve largely mirrors the extent of hydrogen bonds between the methanol molecules (Figure S4b). However, at temperatures lower than 260 K, the energy continues to decrease (larger magnitudes with negative values), whereas the number of hydrogen bonds per molecule hardly exhibits any change from its saturated value of 2. This is likely to be, at least in part, a result of the gain in dipole−dipole energy from the antiparallel ordering.

In this series of simulations we reduced the temperature until 160 K. Experimentally, a monolayer of methanol adsorbed on graphite freezes at 142 K.[23] Analyses of the simulation results indicate that the two-dimensional methanols we studied is in the liquid state above T = 200 and 220 K for the PME and cutoff simulations, respectively. Only at these temperatures does the lateral mean-squared displacement exhibit an onset of the cage-effect (Figure S5) where the dynamics is significantly retarded. These temperatures mark the end-points of the transitions of the antiparallel −OH dipole alignment. The magnitudes of the corresponding diffusion constants (Figure S5c) indicate that the two-dimensional methanols across this transition experience substantial mobility. However, in the vicinity of the low-temperature end, the values of the diffusion constants, which are on the order of 10^{-7} cm^2/s, characterize liquid-crystalline phases;[24,25] therefore, we cannot exclude a transition to such a phase. Note that we did not find any long-range translational order in any of the systems studied (see Figure S6), excluding the possibility of crystallization. Nevertheless, at

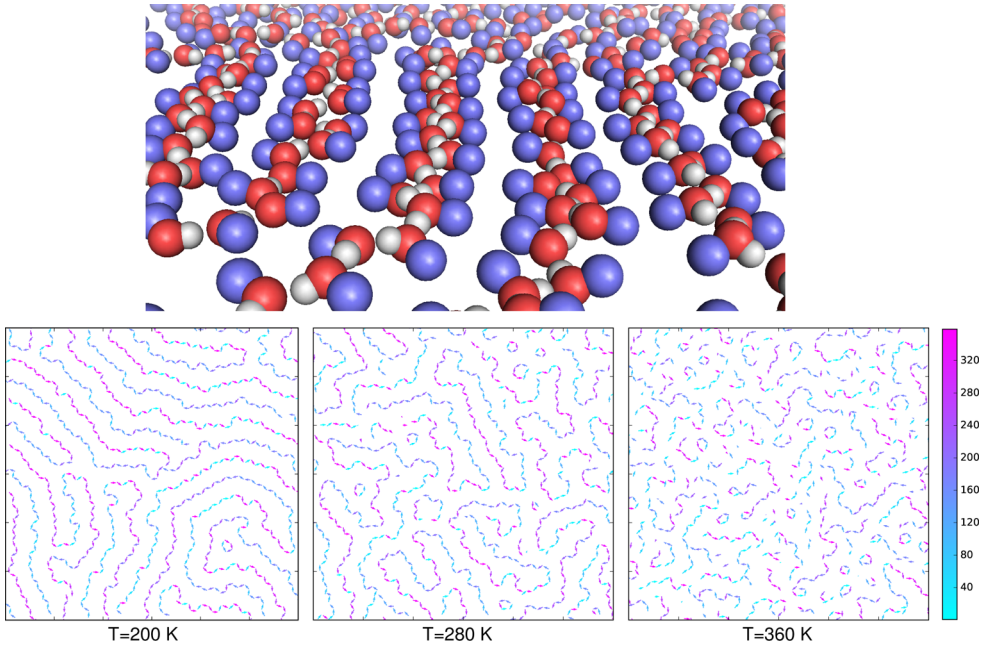

Figure 4. Snapshots from the simulations analyzed in Figure 3. The top panel displays a zoom of a segment of the simulation box (of confined methanols using the cutoff method at ρ_{2D} = 5.76 nm^{-2} and T = 160 K) characterized by the antiparallel ordering of the hydrogen bonds (or molecular) dipoles relative to neighboring (which do not belong to the same chain) hydrogen bonds (molecules). Methyl groups, oxygens, and hydrogens are depicted in blue, red, and white, respectively. The lower panel shows this order−disorder transition by displaying snapshots from three different temperatures. The arrows in the graphs represent the molecular dipole vectors of methanols encoded in a color according to its angle with respect to a fixed coordinate system. The color bar scale is shown on the right.

DOI: 10.1021/acs.nanolett.6b00460
Nano Lett. 2016, 16, 3142−3147

low-temperatures the monolayer does exhibit a large degree of ordering (Figure 4). This apparent discrepancy is because patches of ordered molecules are oriented chaotically with respect to one another. Furthermore, the ordering of the antiparallel strings of methanols does not seem to develop any spontaneous dipole moment in the system at any point along the transition (Figure S7). Thus, in general, the number of strings oriented in one direction is counterbalanced by a similar number of strings oriented in the opposite directions.

Liquids in the vicinity of flat hard surfaces exhibit stratification that extends a few molecular diameters into the bulk.[26,27] At low temperatures, the transverse density of the first layer can have a minimal overlap with the adjacent layer. Does this first layer share similar properties as those found for the confined and adsorbed monolayer systems? To this end, we simulated methanols confined between two graphene sheets with a gap size of about 4 nm (containing 9−10 layers) at different temperatures. The results and instantaneous configurations shown in Figure S8 reveal that the extensive formation of strings reported above does not occur here. Nevertheless, lowering the temperature slightly increases the size of the strings. Furthermore, the values of the order parameter Φ are small: −0.11 and −0.07 for T = 200 and 300 K, respectively. Thus, the interfacial layer of methanol next to a wall is lacking the structural properties of a two-dimensional system. The destruction of structural order is likely to be a result of hydrogen bondings with the adjacent layer.

In this work, two-dimensional methanol systems have been shown to undergo two unique structural organizations that do not have apparent counterparts in three dimensions. The closest analogy in 3D systems is the ordering found in the various liquid crystalline phases in which a significant anisotropy of the molecules is required.[28] In contrast, in two-dimensions a very weak anisotropy is sufficient to introduce self-organization in the gaslike phase or ordering in the liquid (-crystalline) state. This peculiar behavior is likely due to the coupling between the system's reduced dimensionality and the amphiphilic character of methanol. It is yet to be seen what are the consequences of a larger hydrocarbon chain, as is the case for all other alcohols. Note that the results presented in this Letter are applicable to the molecular model of methanol under confinement and therefore require experimental verification. We hope this can be achieved either by using high-resolution transmission electron microscopy[8] or scanning tunneling microscopy imaging.[29,30]

Experimental Section. Condensed phase of methanols in two-dimensions was realized either by confining the molecules between two parallel (and in-registry) graphene sheets, 0.83 nm apart, or by adsorbing the methanols onto a single graphene sheet in vacuum. Graphene was chosen as the confining surface because the methanol molecules are not likely to be commensurate with its structure. The adsorbed methanol system was constructed by placing each of the graphene sheets, together with the associated adsorbed methanols, 10 nm apart such that these two replica of the system effectively did not interact with each other. In both cases, periodic boundary conditions were effectively applied only along the lateral direction (x- and y-axes). Periodicity along the z-axis was suppressed by taking a large (larger than 6 nm) vacuum region above and below the two graphene sheets.

These single-layered graphene sheets, with a fixed dimension of 12.03 × 12.33 nm^2 and consisting of 5684 atoms each, interacted (via bonded and nonbonded interactions) with their periodic images along the lateral direction in such a way that they created an infinite surface. To prevent their translations in the simulation box, the atoms of the graphene sheets were restrained by harmonic potentials in all directions with a force constant of 1000 kJ/(mol·nm^2). The Lennard-Jones (LJ) parameters for the carbon atoms of the graphenes, σ_{CC} = 0.3851 nm and ϵ_{CC} = 0.4396 kJ/mol, were taken from parametrization of single-wall carbon nanotubes[31] with bond stretching and angle bending as detailed in our previous work.[32] The methanol molecules were described by the united-atom OPLS force-field[33] using the geometric combination rules for calculating their interaction with the graphene sheets.

The simulations were performed at constant *NVT* ensemble in two different series. In the first, the number of methanol molecules varied from 36 to 1105 at constant temperature of 300 K. In this case, we presented the state of the system by the two-dimensional number density $\rho_{2D} = N/A$ where A is the lateral area. Because our aim is to investigate the behavior in two dimensions, we restricted the states of the system to those exhibiting only a monolayer of methanols. This was the case for all densities in the confined methanol systems; however, for the adsorbed methanol systems with densities larger than ρ_{2D} = 5.76 nm^{-2}, a second layer starts to develop (see Figure S9). Therefore, these simulations were not processed. This observation is in agreement with an X-ray diffraction study[23] which concluded that at 132 K the monolayer capacity of methanol on graphite is about 6 molecules per nm^2. In the second series of simulations, we varied the temperature in the range of 160 and 440 K at a constant number of methanols, N = 855 (ρ_{2D} = 5.76 nm^{-2}). Bulk methanol boils at 338 K;[34] however, for the adsorbed system at ρ_{2D} = 5.76 nm^{-2}, we did not observe evaporation (except of infrequent instantaneous departures of molecules that could also readsorb at the remote system) even up to T = 360 K. Nevertheless, at this temperature there was also an onset of a bilayer; thus, we did not apply higher temperatures for the adsorbed system in this series of simulations. In Figure S10 we plot the autocorrelation functions between the states of adsorption at different time intervals for ρ_{2D} = 5.76 nm^{-2} at three different temperatures. This density was chosen because it exhibits the fastest decay of adsorbed methanols. The graph indicates that the average lifetime for a methanol molecule on graphene is 2610, 42.5, and 3.7 ns for T = 240, 300, and 360 K, respectively. Thus, for the relevant temperatures, the residence time of the methanols on the surface is much longer than the relaxation times characterizing the different structural orders.

We used the molecular dynamics package GROMACS version 4.6.5[35] to perform all of the computer simulations with a time step of 0.002 ps. The desired temperature was maintained by the velocity rescaling thermostat,[36] applied for the whole system, with a coupling time of 0.1 ps. In light of reports of artifacts that might emerge because of the artificial periodicity imposed by Ewald summation,[37] the simulations were conducted using a cutoff method (twin-ranged of 1.0 and 1.4 nm updated every 1 and 5 steps, respectively) for the calculation of the electrostatics and LJ forces. Nevertheless, the confined methanol system was also simulated using the particle-meshed Ewald (PME) method,[38] adapted for a slab geometry, for comparison. The cutoff distance of the PME real-space part was 1.0 nm and the grid spacing for the reciprocal-space was 0.12 nm with quadratic interpolation. In this case, the LJ potential was evaluated by a single cutoff distance of 1.0 nm. Although quantitative differences were noticed in the calculation

DOI: 10.1021/acs.nanolett.6b00460
Nano Lett. 2016, 16, 3142−3147

of Φ and D_{xy}, qualitatively, these two methods yielded the same results. When using the PME method, long-range electrostatic interactions, and even those from periodic boxes, are taken into account. These excess energetic terms are not likely to be the same for both phases across the transition, and consequently the exact transition point depends on whether they are included or not.

In general, all systems were equilibrated for 80 ns and data collected for additional 80 ns. However, for temperatures below T = 260 K, the systems were further equilibrated for an additional 160 ns. The lateral and transverse pressures were calculated from the corresponding internal virials of the methanol molecules.[39] Note that the graphene sheet is built as a periodic surface; therefore, its virial can not be used to calculate the contribution to the force it exerts on the walls of the simulation box.

The simulations of bulk methanol (in the absence of any confining walls) were performed with 1728 molecules, in a cubic-shaped box, with PME and cutoff methods for calculating the electrostatic forces. Here, in addition to a thermostat, the system was also coupled to a barostat[40] at a pressure of 1.0 bar (with a compressibility of 1×10^{-4} 1/bar and a coupling time of 1.0 ps).

Analysis of the Results. To compute the distributions of strings and rings formed by the methanol molecules, we determined for each molecule the number of contact neighbors and the list of these neighbors. Particles with zero neighbors were labeled as such. We identify first the strings by starting to check particles that have only one contact neighbor. Then, its neighbor is checked. The assignment of the string element continues as long as the next unvisited neighbor has two contact neighbors, and it ends when it has only one neighbor. After all one-neighbor molecules were visited, we start the assignment of rings. To this end, we choose unvisited molecules that have two neighbors and continue to the next unvisited neighbor until we reached a molecule in which all its neighbors were visited. This algorithm unambiguously assigns strings and rings provided the network does not contains particles with more than two neighbors. In all the systems studied, the fraction of particles with more than two neighbors was less than 0.02. When this situation was encountered, we continued with the identification of the structural element toward the neighbor with the shortest contact (as defined by acceptor−donor distance), whereas the remaining branch was considered independently. Two methanol molecules were considered to be in contact if they formed a hydrogen bond with each other. The latter was defined if the donor−acceptor and hydrogen−acceptor distances were simultaneously smaller than 0.35 and 0.25 nm, respectively, and the donor−hydrogen−acceptor angle was larger than 135° (corresponding to the first minimum from linearity in the angle distribution).

■ ASSOCIATED CONTENT

Supporting Information

The Supporting Information is available free of charge on the ACS Publications website at DOI: 10.1021/acs.nanolett.6b00460.

Additional table and figures (PDF)

■ AUTHOR INFORMATION

Corresponding Author

*E-mail: r.zangi@ikerbasque.org.

Notes

The authors declare no competing financial interest.

■ ACKNOWLEDGMENTS

R.Z. acknowledges technical and staff support of the computer cluster provided by IZO-SGI SGIker of UPV/EHU and European funding (ERDF and ESF). D.R. acknowledges the computational resource facilities of Jacobs University Bremen.

■ REFERENCES

(1) Mermin, N. D. *Phys. Rev.* **1968**, *176*, 250−254.
(2) Peierls, R. *Surprises in Theoretical Physics*; Princeton University Press: Princeton, NJ, 1979.
(3) Koga, K.; Zeng, X. C.; Tanaka, H. *Phys. Rev. Lett.* **1997**, *79*, 5262−5265.
(4) Hummer, G.; Rasaiah, J. C.; Noworyta, J. P. *Nature* **2001**, *414*, 188−190.
(5) Zangi, R.; Mark, A. E. *Phys. Rev. Lett.* **2003**, *91*, 025502.
(6) Maniwa, Y.; Kataura, H.; Abe, M.; Udaka, A.; Suzuki, S.; Achiba, Y.; Kira, H.; Matsuda, K.; Kadowaki, H.; Okabe, Y. *Chem. Phys. Lett.* **2005**, *401*, 534−538.
(7) Han, S.; Choi, M. Y.; Kumar, P.; Stanley, H. E. *Nat. Phys.* **2010**, *6*, 685−689.
(8) Algara-Siller, G.; Lehtinen, O.; Wang, F. C.; Nair, R. R.; Kaiser, U.; Wu, H. A.; Geim, A. K.; Grigorieva, I. V. *Nature* **2015**, *519*, 443−445.
(9) Morishige, K.; Kawano, K. *J. Chem. Phys.* **2000**, *112*, 11023−11029.
(10) Morineau, D.; Guégan, R.; Xia, Y.; Alba-Simionesco, C. *J. Chem. Phys.* **2004**, *121*, 1466−1473.
(11) Guégan, R.; Morineau, D.; Alba-Simionesco, C. *Chem. Phys.* **2005**, *317*, 236−244.
(12) Takamuku, T.; Maruyama, H.; Kittaka, S.; Takahara, S.; Yamaguchi, T. *J. Phys. Chem. B* **2005**, *109*, 892−899.
(13) Gupta, N. M.; Kumar, D.; Kamble, V. S.; Mitra, S.; Mukhopadhyay, R.; Kartha, V. B. *J. Phys. Chem. B* **2006**, *110*, 4815−4823.
(14) Chaban, V. V.; Kalugin, O. N. *J. Mol. Liq.* **2009**, *145*, 145.
(15) Zang, J.; Konduri, S.; Nair, S.; Sholl, D. S. *ACS Nano* **2009**, *3*, 1548−1556.
(16) Elola, M. D.; Rodriguez, J.; Laria, D. *J. Chem. Phys.* **2010**, *133*, 154707.
(17) Garberoglio, G. *J. Phys.: Condens. Matter* **2010**, *22*, 415104.
(18) Yamaguchi, T.; Hidaka, K.; Soper, A. K. *Mol. Phys.* **1999**, *96*, 1159−1168.
(19) Tauer, K. J.; Lipscomb, W. N. *Acta Crystallogr.* **1952**, *5*, 606−612.
(20) Magini, M.; Paschina, G.; Piccaluga, G. *J. Chem. Phys.* **1982**, *77*, 2051−2056.
(21) Torrie, B. H.; Weng, S. X.; Powell, B. M. *Mol. Phys.* **1989**, *67*, 575−581.
(22) Robyr, P.; Meier, B. H.; Fischer, P.; Ernst, R. R. *J. Am. Chem. Soc.* **1994**, *116*, 5315−5323.
(23) Morishige, K.; Kawamura, K.; Kose, A. *J. Chem. Phys.* **1990**, *93*, 5267−5270.
(24) Medina, I. *Chromatographia* **1993**, *35*, 539−542.
(25) Dvinskikh, S. V.; Furó, I.; Zimmermann, H.; Maliniak, A. *Phys. Rev. E: Stat. Phys., Plasmas, Fluids, Relat. Interdiscip. Top.* **2002**, *65*, 061701.
(26) Abraham, F. F. *J. Chem. Phys.* **1978**, *68*, 3713−3716.
(27) Israelachvili, J. N.; McGuiggan, P. M.; Homola, A. M. *Science* **1988**, *240*, 189−191.
(28) de Gennes, P. G.; Prost, J. *The Physics of Liquid Crystals*; Clarendon Press: Oxford, 1993.
(29) Yang, T.; Berber, S.; Liu, J.-F.; Miller, G. P.; Tománek, D. *J. Chem. Phys.* **2008**, *128*, 124709.
(30) Zhang, T.; Cheng, Z.; Wang, Y.; Li, Z.; Wang, C.; Li, Y.; Fang, Y. *Nano Lett.* **2010**, *10*, 4738−4741.

DOI: 10.1021/acs.nanolett.6b00460
Nano Lett. 2016, 16, 3142−3147

(31) Walther, J. H.; Jaffe, R.; Halicioglu, T.; Koumoutsakos, P. *J. Phys. Chem. B* **2001**, *105*, 9980−9987.
(32) Sarukhanyan, E.; Milano, G.; Roccatano, D. *J. Phys. Chem. C* **2014**, *118*, 18069−18078.
(33) Jorgensen, W. L.; Maxwell, D. S.; Tirado-Rives, J. *J. Am. Chem. Soc.* **1996**, *118*, 11225−11236.
(34) Goodwin, R. D. *J. Phys. Chem. Ref. Data* **1987**, *16*, 799−892.
(35) Hess, B.; Kutzner, C.; van der Spoel, D.; Lindahl, E. *J. Chem. Theory Comput.* **2008**, *4*, 435−447.
(36) Bussi, G.; Donadio, D.; Parrinello, M. *J. Chem. Phys.* **2007**, *126*, 014101.
(37) Hünenberger, P. H.; McCammon, J. A. *Biophys. Chem.* **1999**, *78*, 69−88.
(38) Darden, T.; York, D.; Pedersen, L. *J. Chem. Phys.* **1993**, *98*, 10089−10092.
(39) Zangi, R.; Rice, S. A. *Phys. Rev. E: Stat. Phys., Plasmas, Fluids, Relat. Interdiscip. Top.* **1998**, *58*, 7529−7544.
(40) Berendsen, H. J. C.; Postma, J. P. M.; van Gunsteren, W. F.; DiNola, A.; Haak, J. R. *J. Chem. Phys.* **1984**, *81*, 3684−3690.

DOI: 10.1021/acs.nanolett.6b00460
Nano Lett. 2016, 16, 3142−3147

Supporting Information:

Strings-to-Rings Transition and Anti-parallel Dipole Alignment in Two-Dimensional Methanols

Ronen Zangi[1,2] and Danilo Roccatano[3,4]

[1]Polymat & Department of Organic Chemistry I, University of the Basque Country UPV/EHU, Avenida de Tolosa 72, 20018, San Sebastian, Spain

[2]IKERBASQUE, Basque Foundation for Science, Maria Diaz de Haro 3, 48013 Bilbao, Spain

[3]School of Mathematics and Physics, University of Lincoln, Brayford Pool, Lincoln, LN6 7TS, UK

[4]School of Engineering and Science, Jacobs University Bremen, Campus Ring 1, 28759 Bremen, Germany

April 5, 2016

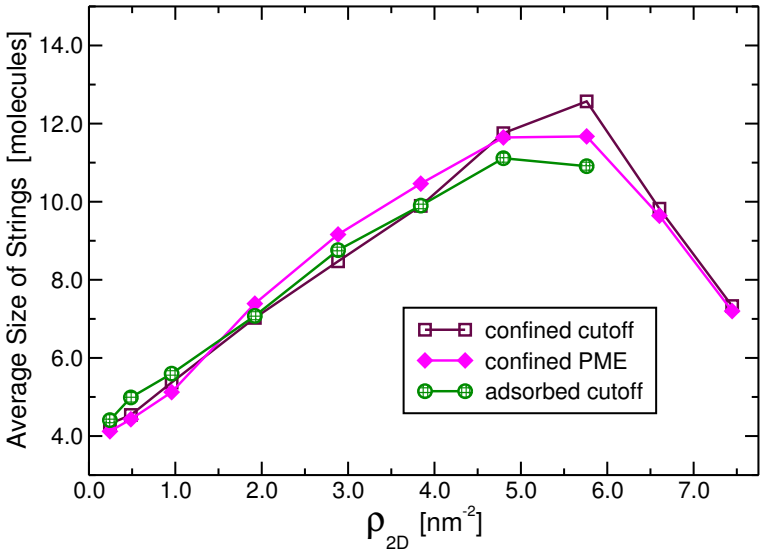

Figure S1: The average size of the string structural element as a function of the two dimensional density for the three systems analyzed in Fig. 1.

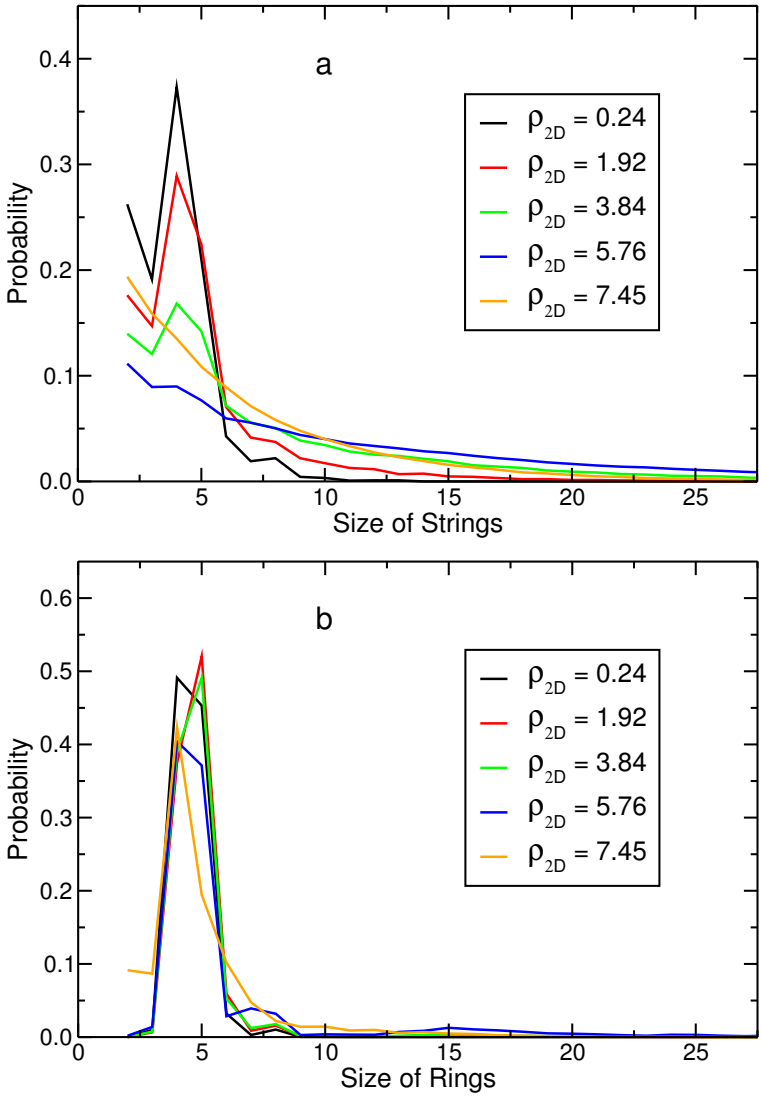

Figure S2: Normalized distributions of (a) strings and (b) rings structural elements for the confined methanol systems using the cutoff method. Very similar distributions are obtained from the PME method, as well as, when the methanols are adsorbed on a single graphene sheet. Note that the large peaks for strings with sizes 4 and 5 at low densities are due to rings elements that are transiently broken by thermal fluctuations.

Table S1: The percentage of particles participating in 4- and 5-member-rings from all particles assigned to rings structural elements for the systems analyzed in Fig. 1. In each case, the first and the second numbers correspond to the results of the confined methanols obtained by PME and cutoff methods, respectively, whereas the third number corresponds to the system in which the methanols are adsorbed on a single graphene sheet.

ρ_{2D} [nm^{-2}]	4-member	5-member	Other rings
0.24	54 / 49 / 41	41 / 45 / 51	5 / 6 / 8
0.49	47 / 42 / 34	47 / 52 / 56	6 / 6 / 10
0.96	42 / 39 / 36	51 / 52 / 52	7 / 9 / 12
1.92	39 / 37 / 33	52 / 52 / 53	9 / 11 / 14
2.88	39 / 37 / 33	51 / 51 / 51	10 / 12 / 16
3.84	39 / 39 / 34	51 / 49 / 49	10 / 12 / 17
4.80	40 / 39 / 34	47 / 47 / 45	13 / 14 / 21
5.76	39 / 40 / 29	42 / 37 / 38	19 / 23 / 33
6.60	40 / 39 / –	26 / 25 / –	34 / 36 / –
7.45	43 / 42 / –	21 / 19 / –	36 / 39 / –

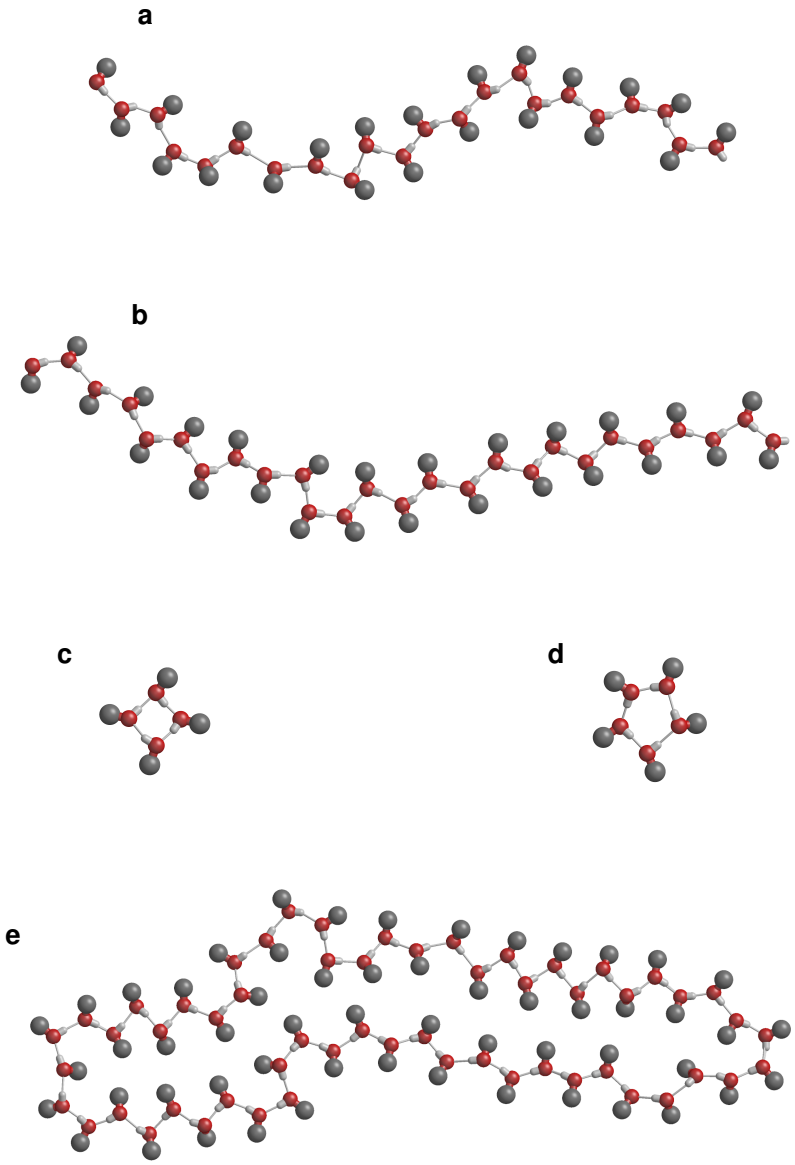

Figure S3: Three representative structural elements. (a) A string at T=300 K, (b) a string at T=200 K, (c) a four-member ring, (d) a five-member ring, and (e) a large ring composed of a string in which its ends are connected to each other.

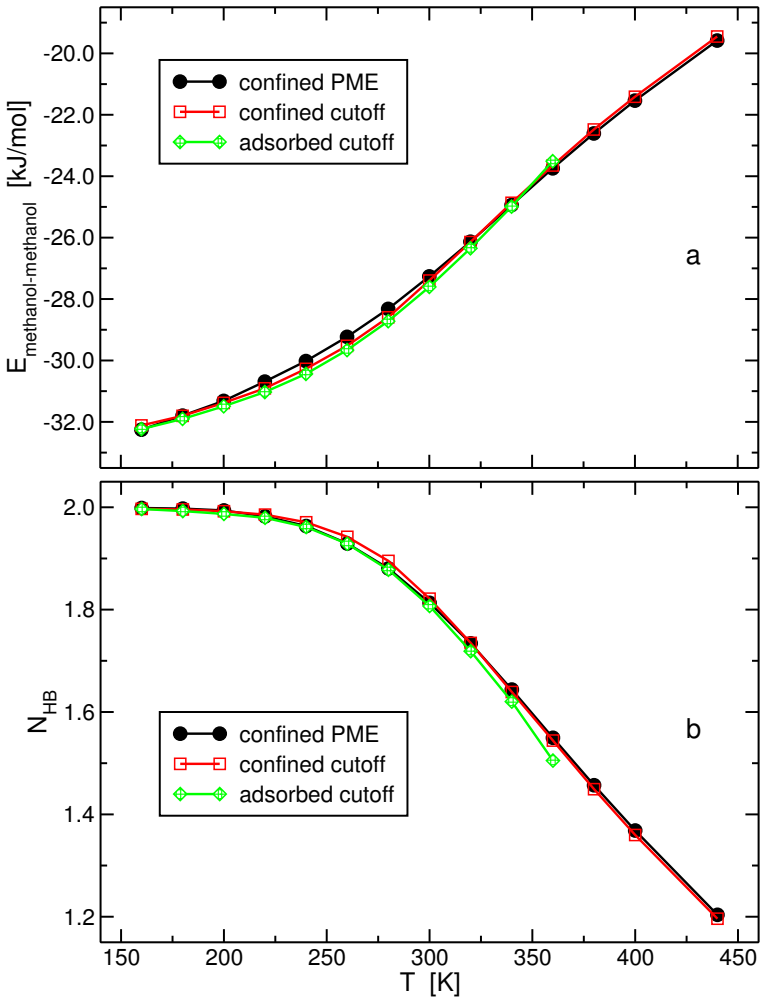

Figure S4: (a) The methanol-methanol potential energy per molecule, and (b) the number of hydrogen bonds each methanol forms with its neighbors, as a function of temperature for the three two-dimensional methanol systems studied.

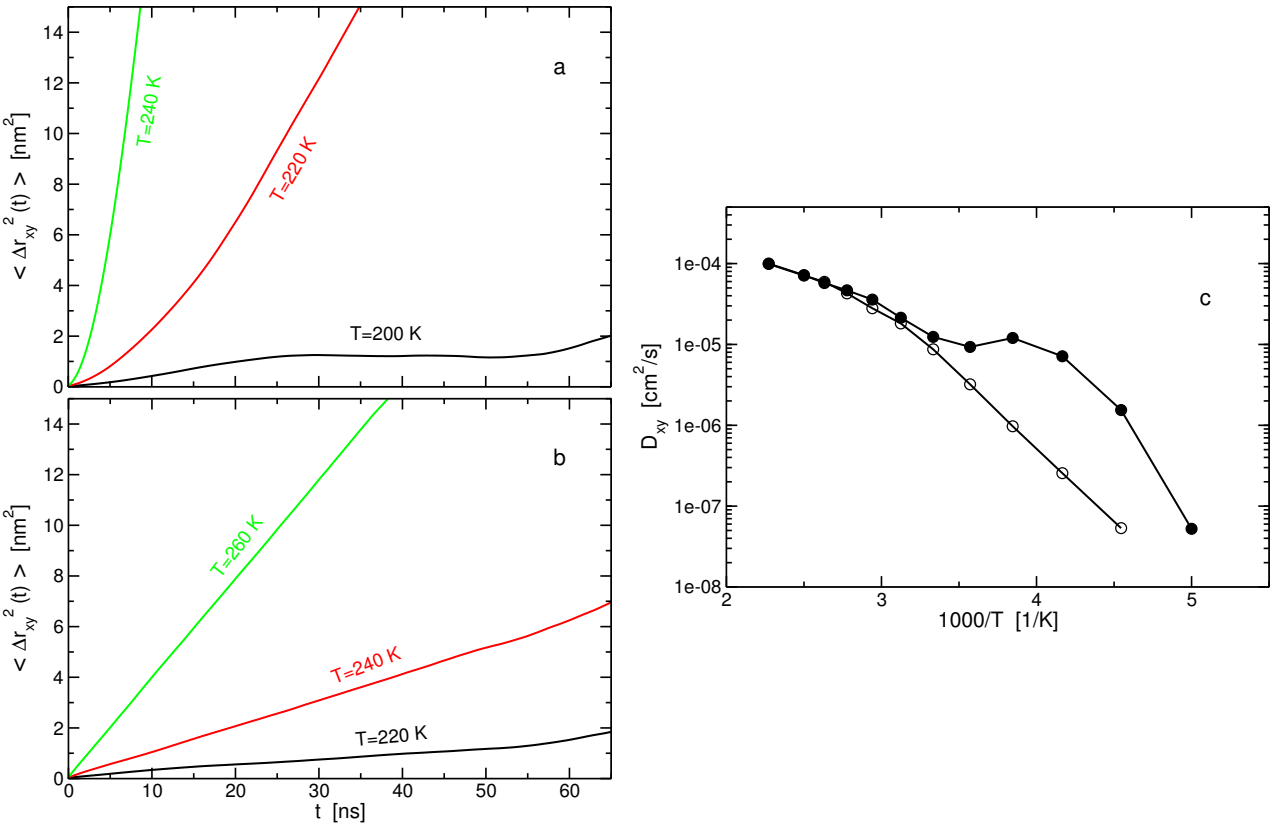

Figure S5: (a) The mean-squared displacement of methanols in the xy-plane as a function of time at T=200, 220, and 240 K for the confined methanol system using the PME method. (b) Same as (a) but for the confined methanol system using the cutoff method at T=220, 240, and 260 K. (c) The lateral diffusion constants as a function of inverse temperature (down to temperatures for which diffusion constant can be defined). Filled and empty circles are for the simulations with the PME and cutoff methods, respectively.

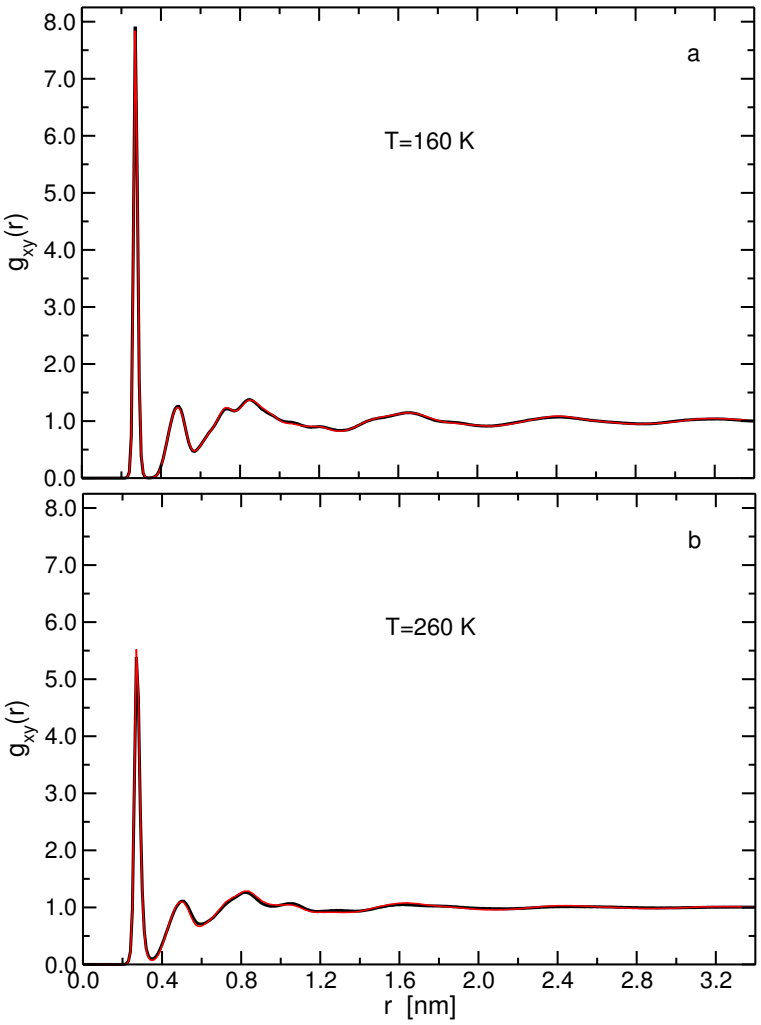

Figure S6: The lateral radial distribution function between the oxygen atoms for the confined methanol system at (a) T=160 K and (b) T=260 K. Black and red curves (which are almost indistinguishable) correspond to results from simulations in which the electrostatics were calculated using PME and cutoff methods, respectively.

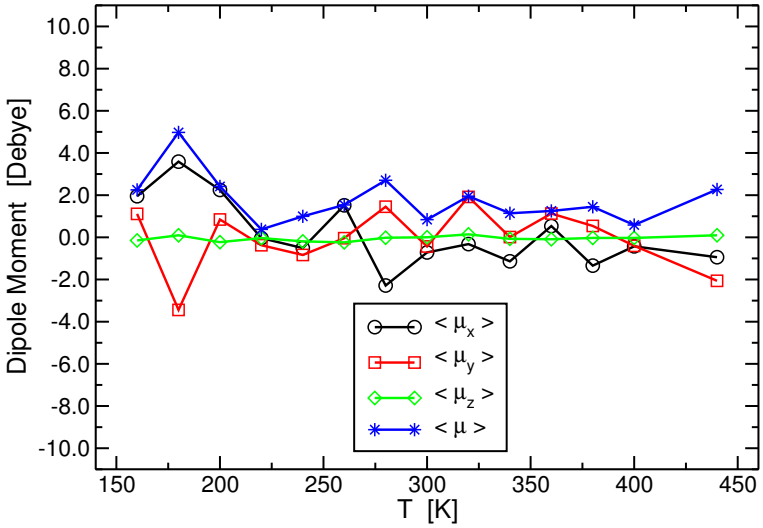

Figure S7: The total dipole moment of the entire system and its three Cartesian coordinates as a function of temperature for the confined methanol system using the cut-off method.

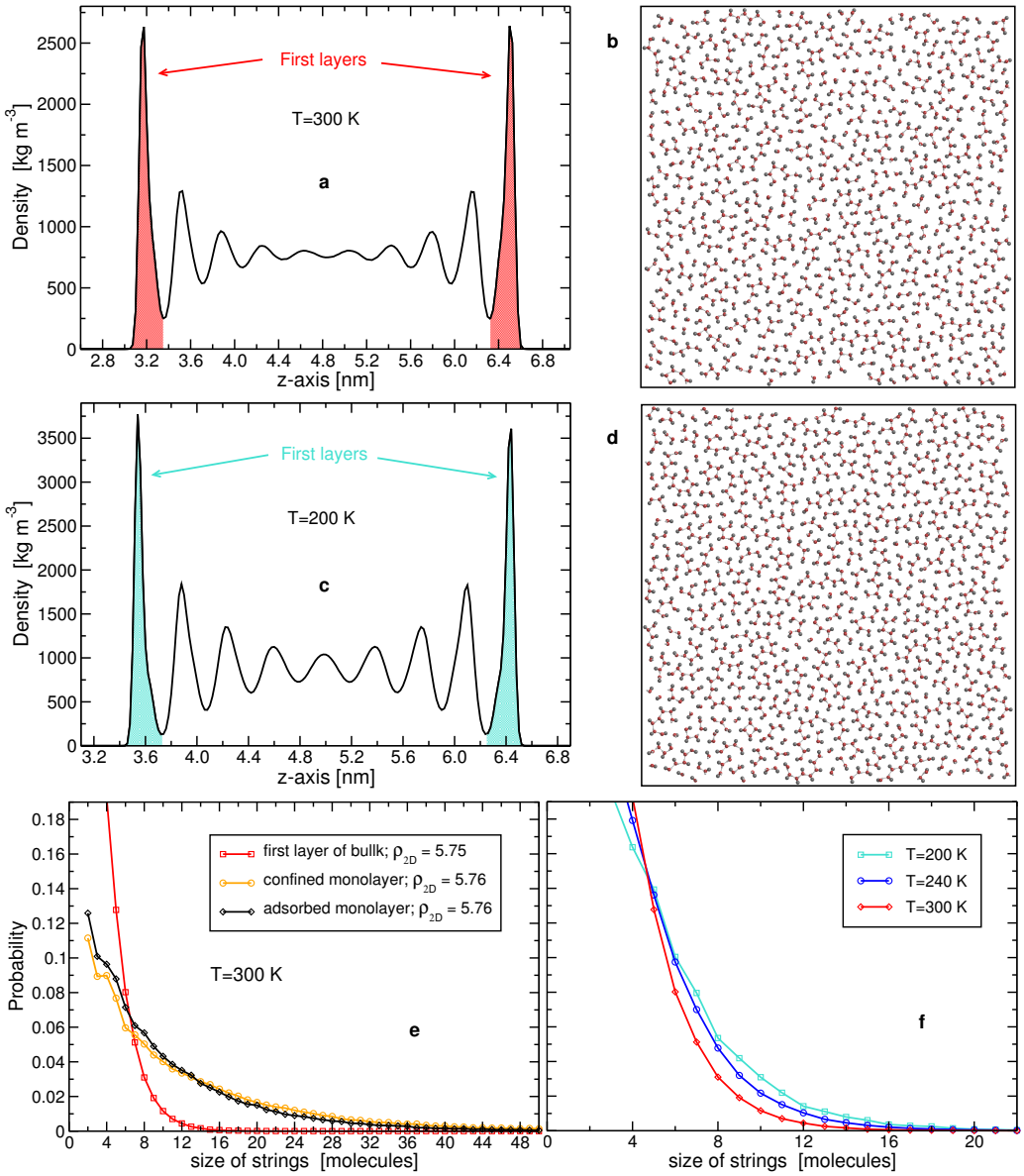

Figure S8: Results from simulations with 8170 methanols in which the gap between the confining graphene sheets is: 4.1, 3.8 and 3.6 nm at T=300, 240, and 200 K, respectively. The gap size was chosen such that the density of methanols farther away from the graphenes is the same as the corresponding bulk density (the resulting lateral or transverse pressure ranged from 4.1 to 5.5 bar). (a) and (c) The density profiles of methanols along the z-axis, and (b) and (d) snapshots of one of the first layers of methanol from the graphene surfaces. (e) The normalized distributions of the string size for a monolayer of methanol under different constraints at T=300 K. (f) Same as (e) but for the first interfacial layers of bulk (in systems in which the confining graphenes allow the existence of 9–10 methanol layers).

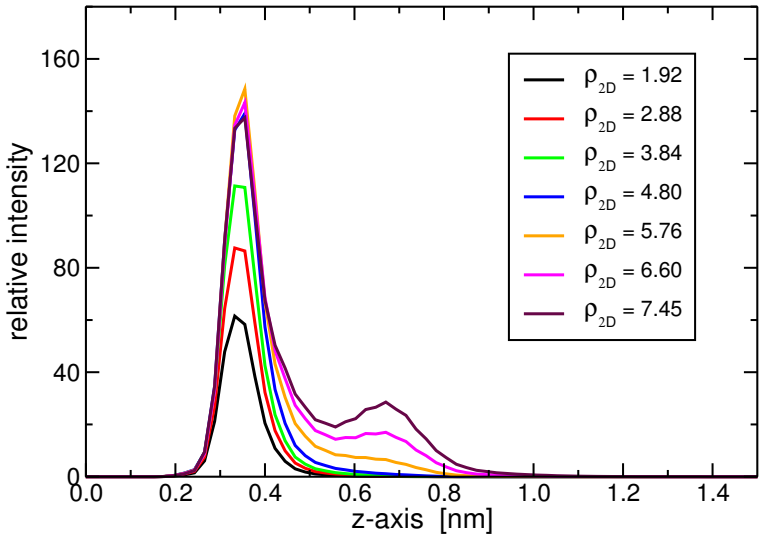

Figure S9: The density of methanols (counted by the molecule center of mass in relative numbers) adsorbed on the graphene sheet along its surface normal (z-axis) for the high-end two-dimensional densities studied. Note that at the two largest densities, there is a clear onset of a bilayer, and therefore, the data obtained from these simulations were not considered further.

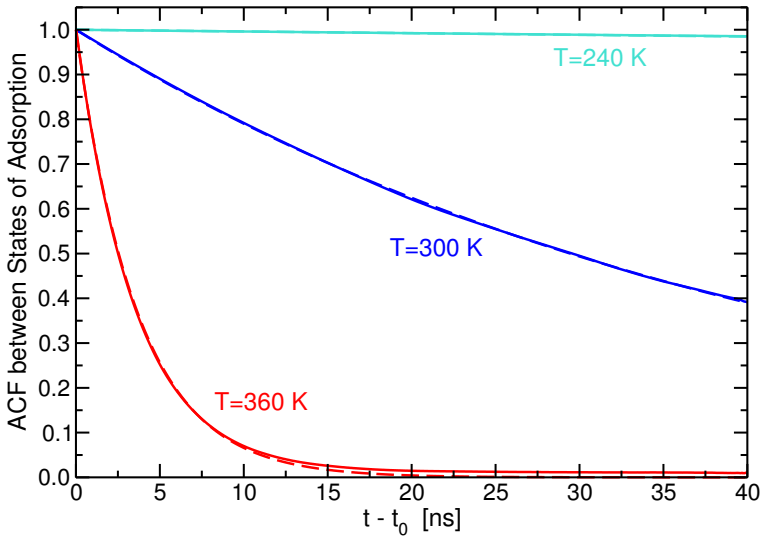

Figure S10: The normalized adsorption auto-correlation function for the simulations of methanols adsorbed on a single graphene sheet for ρ_{2D}=5.76 nm^{-2} at three different temperatures. The fit exponential decays are also plotted as dashed lines in the same colors as the auto-correlation functions (however, they are hardly visible due to overlaps). The resulting decay constants are 0.272, 2.35·10^{-2}, and 3.83·10^{-4} ns^{-1} for T=360, 300, and 240 K, respectively. The adsorption auto-correlation function is defined as $\langle \frac{1}{N} \sum_{i=1}^{N} \phi_{\text{ads,i}}(t;t_0) \cdot \phi_{\text{ads,i}}(t_0) \rangle$ where the sum is performed over all N methanol molecules and the angle brackets denote an average over all possible time intervals, $t - t_0$, in the trajectory. $\phi_{\text{ads,i}}(t;t_0)$ equals one when methanol i had been continuously adsorbed to the graphene sheet from time t_0 until time t, otherwise it equals zero. Adsorption is determined by a cut-off distance of 0.9 nm along the z-axis between the oxygen atom of methanol and the closest carbon atom of the graphene sheet.